

## A Comparative Study on the Corrosion of Galvanized Steel under Simulated Rust Layer Solution with and without 3.5wt%NaCl

Huyuan Sun<sup>1,\*</sup>, Shuan Liu<sup>1,2,\*</sup>, Lijuan Sun<sup>1</sup>

<sup>1</sup> Institute of Oceanology, Chinese Academy of Sciences, Qingdao 266071, China;

<sup>2</sup> Graduate University of Chinese Academy of Sciences, Beijing 100049, China

\* E-mail: [Sun@qdio.ac.cn](mailto:Sun@qdio.ac.cn); [shuanzi123456@yahoo.com.cn](mailto:shuanzi123456@yahoo.com.cn)

Received: 4 January 2013 / Accepted: 10 February 2013 / Published: 1 March 2013

---

A comparative study of the corrosion behavior of galvanized steel under 3.5wt% NaCl and chloride-free simulated rust layer (SRL) solution was investigated using polarization curve and electrochemical impedance spectroscopy (EIS). The morphology, organization and chemical properties of the rust layer were detected by scanning electron microscopy (SEM), X-ray diffraction (XRD) and energy dispersive spectroscopy (EDS). The results indicated that the rust layer could inhibit the corrosion of galvanized steel in chloride-free SRL solution, both of the resistance of rust layer ( $R_f$ ) and charge transfer resistance ( $R_{ct}$ ) increased with the increase of immersion time. However, non-uniform corrosion occurred on the galvanized steel in the SRL solution containing 3.5wt% NaCl, the rust layer absorbed on the electrode was gradually destroyed under the erosion of  $Cl^-$ .

---

**Keywords:** corrosion behavior; galvanized steel; simulated rust layer;  $Cl^-$

### 1. INTRODUCTION

Galvanized steel is widely used in the applications such as building, automotive body parts and water distribution systems because of its good resistance to environmental corrosion [1-4]. The protection obtained by zinc coating is due to barrier and galvanic double protective effect [5-6]. However, many cases of heavy damage of galvanized pipes and tanks have been reported as being due to corrosion processes in water hanging system, as clearly evidenced by the production of rust layer in those systems after an unexpectedly short lifetime [7].

Rust/metal structure is one of the multiphase and multiple interface complex systems. The corrosion under rust layer is the uppermost and longest form of the metallic corrosion evolution. Many atmospheric corrosion studies have established that the composition of the rust layer on galvanized

steel depends on the exposure conditions, type and level of the pollutants, and the number of the wet-dry cycles [8-10]. In an unpolluted aqueous solution, ZnO and Zn(OH)<sub>2</sub> are the most abundant corrosion products[11-12]. The rust layer absorbed on the zinc coating surface would affect corrosion-related processes, such as the mass transport of dissolved oxygen, the stability of the passive film and the hydration of the dissolved metal ions. Besides, the corrosion reactions under rust layer are not only simple reactions including metal anodic dissolution and oxygen reduction, but also complex corrosion process composed of multiple sub-processes involving rust redox reactions, mass transportation through rust, electric charges movement between interfaces, microorganism propagation in porous rust and some other complex corrosion processes[13-16]. Tsuru [17] proposed that zinc ion dissolved from the rust layer on galvanized steel preventing further corrosion of the steel substrate. He demonstrated the contribution of the zinc-containing rust layer to the corrosion retardation for the Fe substrate, as well as the high sacrificial anode effect of the metallic zinc. Cachet [18,19] investigated the dissolution and corrosion mechanism of high purity zinc in an aerated sulfate medium by using electrochemical impedance analysis and by modeling the process. There were three parallel paths of zinc dissolution and three adsorbed intermediates ( $Zn_{ad}^+$ ,  $Zn_{ad}^{2+}$  and  $ZnOH_{ad}$ ) during the anodic dissolution process. Both of the surface preparation conditions and the rust layer adsorbed on the electrode surface would affect the balance between the competitive dissolution.

The good corrosion resistance of zinc coating is improved when the zinc is alloyed with other metal (e.g. Co, Ni, Mn, Al) [20-22]. Some researchers have suggested that the higher protective ability of these systems is due to the corrosion products, zinc hydroxide salts (Zn(OH)<sub>2</sub>), that formed as a result of interaction with the corrosion medium[23]. In addition, Deslouis[24] proposed that during the corrosion of zinc in an aerated, neutral 0.5 M Na<sub>2</sub>SO<sub>4</sub> solution, a passivation layer, which is composed of ZnO in association with Zn(OH)<sub>2</sub>, formed on the surface of zinc. However, Boshkov [25] found that zinc coatings do not have a passivating effect in an aerated 5 wt% NaCl solution. It is a matter of fact that the corrosion current and corrosion potential are sensitive to the zinc surface conditions as well as to the environment factors (pH of the solution, dissolved oxygen concentration, Cl<sup>-</sup> ion concentration, temperature, et al). These factors have been related to the presence of oxidized species (oxide, hydroxide and carbonate) because of the contact with aqueous solution and to the contribution of the cathodic reduction of dissolved oxygen.

In this paper, saturated Zn(OH)<sub>2</sub> was used to simulate rust layer (SRL) solution, and more Zn(OH)<sub>2</sub> precipitation was added into the test solution to simulate the rusty environment. The corrosion behavior of galvanized steel was studied by electrochemical measurements. Our research work has been focused on the electrochemical and surface studies of the Zn coating exposed to seawater [26]. We also have analyzed the degradation of galvanized steel under different Cl<sup>-</sup> environment [27]. The aim of the present investigation was established for a comparison of the protective properties of rust layer on galvanized steel under 3.5wt% NaCl and chloride-free SRL solution. Especially, the evolution of EIS characteristics of the different immersion time was discussed in details, and the morphology of corrosion products in different periods were imaged by SEM. It is anticipated that this research will provide the essential insight on the corrosion mechanism of galvanized steel under simulated rust layer solution.

## 2. EXPERIMENTAL PROCEDURE

### 2.1. Sample and SRL solution preparation

Galvanized steel sheet was purchased from Shanghai BaoSteel and cut into 3 cm × 3 cm used in the experiments. The actual chemical composition (wt%) of the zinc coating was listed in Table 1. Corrosion experiments were conducted on electrodes made from galvanized steel, cold mounted in epoxy resin to give an exposed area of 1 cm<sup>2</sup> to the medium. A copper wire was lead to the backside of each specimen with a round paste. Before each experiment, the working surface of the electrodes was degreased with ethanol, cleaned with distilled water, and finally dried in air.

**Table 1.** Chemical composition of the zinc coating

Element	C	Mn	P	S	Ti	Zn
Content (wt%)	≤0.04	≤0.20	≤0.011	≤0.008	≤0.036	Balance

In this paper, saturated Zn(OH)<sub>2</sub> solution was used to simulate the rust layer solution. Excessive analytical-grade Zn(OH)<sub>2</sub> was added to maintain its saturation. pH of the SRL solution was 8.42, and the Cl<sup>-</sup> concentration in the SRL solution was maintained by adding NaCl.

### 2.2 Electrochemical measurements

Electrochemical measurements were carried out in a conventional three-electrode glass cell with a platinum counter electrode and a saturated calomel electrode (SCE) as reference. All the potentials in this paper are reported in the SCE scale. The electrochemical cell was prepared by placing the samples horizontally looking upwards at the bottom. The volume of the cell was 400 ml. The galvanized steel was immersed in SRL solution and allowed to attain a stable open circuit potential (OCP) before starting the polarization scan. The polarization curves were recorded by changing the electrode potential automatically with an EG&G 2273 potentiostat, at a scan rate of 0.5 mV/s. All the tests were performed at room temperature (25 °C).

For the cyclic polarization curves, the polarization curves were plotted by starting scanning electrode potential from an initial potential of 250 mV below the open circuit potential (OCP), the scan direction was reversed when the electrode potential reached the anodic potential of 0 V and then the potentials were scanned back to the initial potential. A vertex current density of 0.001 A/cm<sup>2</sup> was used. The EIS measurements were carried out using ac signals of amplitude 10 mV peak to peak at OCP in the frequency range of 100 kHz to 10 mHz. Zview software was used to analyze the EIS data with equivalent circuit.

### 2.3 Observation and characterization of corrosion products

XRD analysis was used to determine the corrosion products formed on the zinc coating under different conditions. An X-ray diffractometer with Cu  $k\alpha$  radiation ( $\lambda = 0.154$  nm) and  $10^\circ$ - $80^\circ$  scanning range was used to obtain XRD patterns from the powder scraped from the surface of the specimens. The microstructure of the corrosion products absorbed on the surface of electrode were observed and recorded by using a KYKY-2800B SEM, and the field emission energy was 10 keV. The chemical composition of the corrosion products was determined using a GENESIS 4000 energy dispersive spectroscopy (EDS) attached to the SEM.

## 3. RESULTS AND DISCUSSION

### 3.1 The polarization curves measurements

The important information on the kinetics of anodic reaction and cathodic reaction could be directly obtained from the polarization curve [28]. At least three parallel polarization tests are carried out for each condition at different immersion times. The average values are given in Table 2. The polarization curves of galvanized steel immersed in 3.5wt% NaCl and chloride-free SRL solution are showed in Fig.1, which is consistent with the previous work conducted in neutral freshwater solution [27].

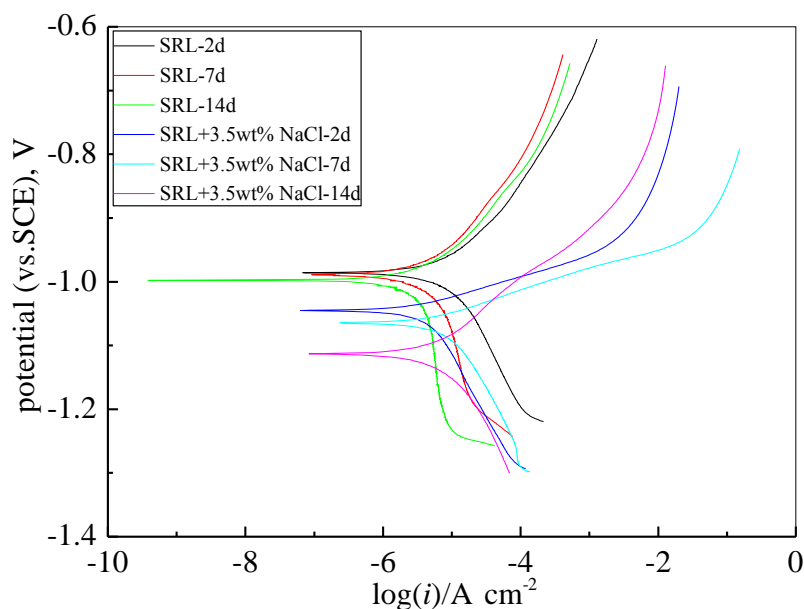


**Figure 1.** Polarization curves of galvanized steel in 3.5wt% NaCl and chloride-free SRL solution

**Table 2.** Electrochemical parameters of the specimens obtained in 3.5wt%NaCl and chloride-free SRL solution

	$E_{corr}$ (V/SCE)	$i_{corr}$ ( $\mu\text{A cm}^{-2}$ )	$\beta_a$ (mV/dec)	$\beta_c$ (mV/dec)
SRL ---2 d	-0.983	5.23	186.3	523.6
SRL ---7 d	-0.985	4.82	176.7	746.2
SRL ---14 d	-0.977	4.63	123.5	910.1
SRL+3.5wt%NaCl---2 d	-1.049	10.62	41.3	198.8
SRL+3.5wt%NaCl---7 d	-1.065	12.54	46.8	172.3
SRL+3.5wt%NaCl---14d	-1.116	14.71	58.2	180.9

It can be observed from the Fig.1 that the  $\text{Cl}^-$  affected remarkably the electrochemical behavior of galvanized steel in SRL solutions. As indicated by the Tafel slopes, the corrosion rates of galvanized steel in both 3.5wt% NaCl and chloride-free SRL solution were found to be under cathodic control (oxygen diffusion control). This was confirmed by the shape of the polarization curves in the SRL solution. In the chloride-free SRL solution, the cathodic polarization curves basically unchanged with time, in combination with the unchangeable  $i_{corr}$ , indicating that the rust layer could inhibit the corrosion of zinc coating to some extent. However, the slopes of branches of the cathodic portion and anodic portion changed greatly in the SRL solution containing 3.5wt% NaCl. The corrosion potential ( $E_{corr}$ ) shifted towards more negative values suggesting further degradation of the zinc coating than that in chloride-free SRL solution. Both of the values of  $\beta_a$  and  $\beta_c$  were smaller than that of the chloride-free SRL solution, the corrosion current ( $i_{corr}$ ) also increased with time. This phenomenon can be explained as followed:  $\text{Cl}^-$  is a strong anodic activator because of its smallest radius and volume, so it can penetrate from the rust layer, destruct the structure of the rust layer and react with the substrate metal directly. After the  $\text{Cl}^-$  destroyed some of the rust layer, the zinc coating appeared and acted as an anode, and the others of the intact rust layer acted as a cathode. Thus, there formed an activation-inactivation corrosion cell. Owing to the smaller anode vs. the larger cathode, this will result in accelerating the pitting corrosion [29]. Therefore, there was remarkable higher corrosion rate of galvanized steel in SRL solution containing 3.5wt% NaCl.

### 3.2 The cyclic polarization curve measurement

One of the electrochemical measurements to assess the sensitivity of galvanized steel to pitting corrosion is the cyclic polarization technique at low scan rate during the initial reaction stage. The cathodic scan provides no information concerning pitting corrosion susceptibility, but it is useful as a final cleaning step. However, pitting corrosion susceptibility can be predicted reliably from the anodic portion of a scan. If the reverse anodic curve is shifted to higher currents than the forward curve (positive hysteresis), pitting is expected. In contrast, if the reverse anodic curve is shifted to lower currents (negative hysteresis) or if the reverse curve essentially retraces the ascending curve (neutral hysteresis), no pitting is expected [30].

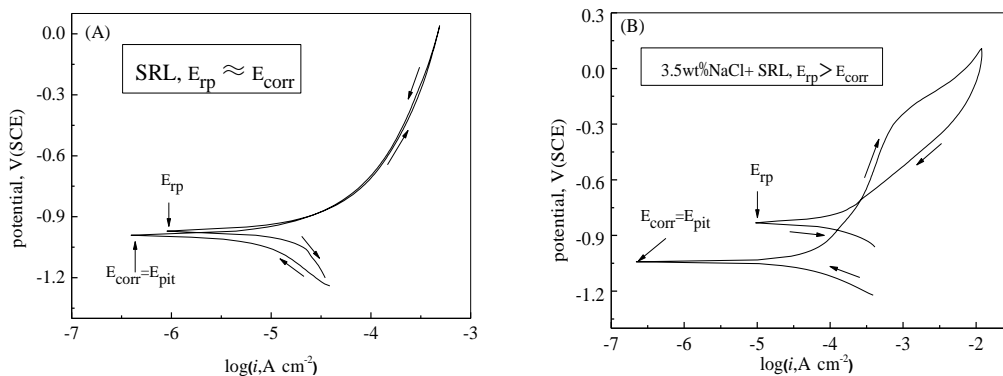
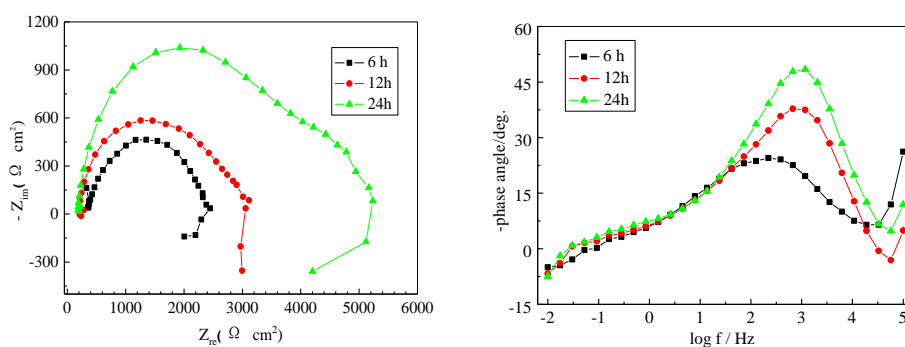


**Figure 2.** Cyclic polarization curves of galvanized steel in SRL solution, (A): chloride-free; (B): 3.5wt% NaCl

The typical cyclic polarization curves of galvanized steel in 3.5wt% NaCl and chloride-free SRL solutions (pH 8.42) are shown in Fig.2, respectively. The solid arrows next to the forward indicate potential scan directions. In the SRL solution, Fig.2 (A) shows a situation of neutral hysteresis, no pitting corrosion occurred on the electrode. The specimen did not show a classical passive region with the current density totally independent of applied potential. The current density increased abruptly until it reached the value of 10<sup>-4</sup> A/cm<sup>2</sup> and then it continued to increase slowly as the potential applied was increased. The highest polarization was near 0 V vs. SCE. However, in the SRL solution containing 3.5 wt% NaCl, Fig.2 (B) shows a situation of positive hysteresis, with pitting potential located at the same position of that of the corrosion potential, repassivation potential  $E_{tp}$  was more positive than  $E_{corr}$  and small area of the hysteresis loop, indicating that nucleation and growth of pitting corrosion on the electrode surface during the reverse scan [27, 31]. After the test, the examined specimens showed the same morphology of the attack by pitting, as that observed on the following SEM images.

### 3.3 The EIS measurements

#### 3.3.1 In chloride-free SRL solution



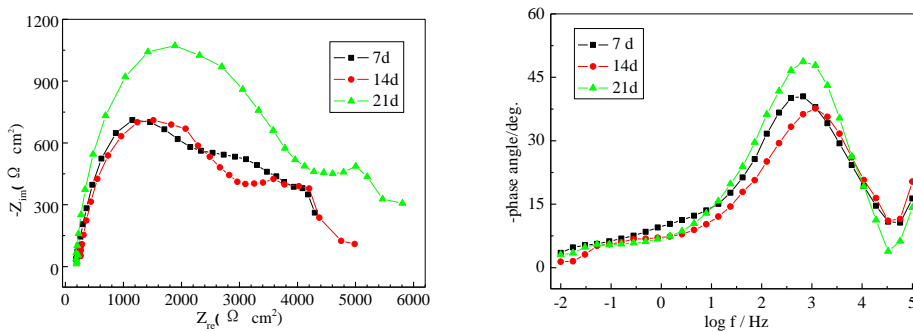


Figure 3. Experimental Nyquist and Bode plots of galvanized steel in chloride-free SRL solution

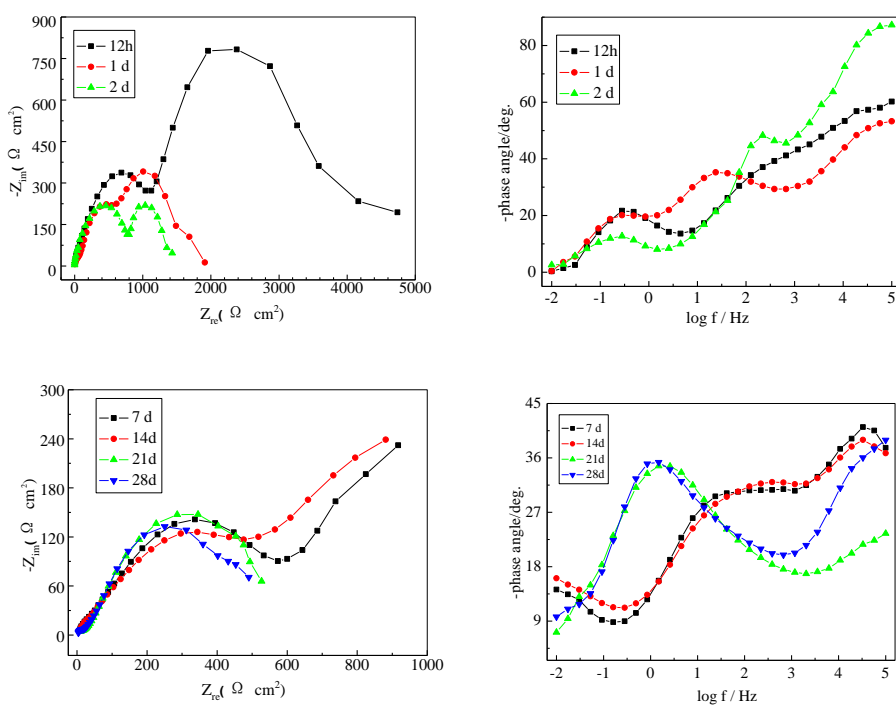


Figure 4. Experimental Nyquist and Bode plots of galvanized steel in SRL solution containing 3.5wt% NaCl

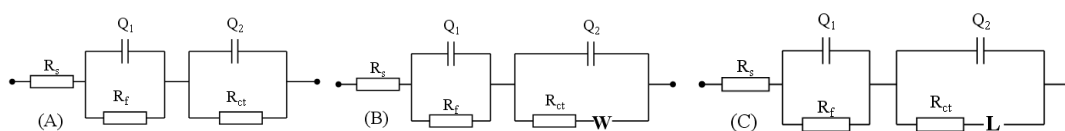


Figure 5. Equivalent circuit of the galvanized steel in SRL solution

EIS is a powerful tool to study the kinetics of electrode reaction processes, which not only provides a non-destructive assessment of the corrosion rate, but also enables the determination of the corrosion mechanism [32-33].

Fig.3 and Fig.4 show the Nyquist and Bode diagrams of galvanized steel exposure to 3.5wt% NaCl and chloride-free SRL solution for different immersion times, respectively. To obtain the electrochemical parameters, three kinds of equivalent circuits in Fig.5 are used to fit the EIS data of galvanized steel in different corrosion mediums, respectively. The corresponding electrochemical parameters of the elements are listed in Table 3 and Table 4. In the three equivalent circuit models, Q is the constant phase angle element, expressed as  $\omega^{-n}/Y_0 \cdot (\cos n\pi/2 + j \sin n\pi/2)$ .  $R_s$  is the solution resistance of the SRL solution, the high-frequency circuit  $R_f \sim Q_1$  correspond to the capacitance and resistance of the surface film of corrosion products; the medium-low frequency circuit  $R_{ct} \sim Q_2$  are the double-layer capacitance and charge transfer resistance, while the W represents the Warburg diffusion impedance and L represents the adsorption of surface species appearing in the low-frequency region, respectively. For the capacitive loops, the coefficients  $n_1$  and  $n_2$  represent a depressed feature in the Nyquist diagram.

**Table 3.** The electrochemical parameters of the EIS in 3.5wt% NaCl SRL solution with different time

T days	$R_s$ $\Omega \text{ cm}^2$	$Q_1$ $\mu\text{F cm}^{-2} \text{ Hz}^{1-n_1}$	$n_1$	$R_f$ $\Omega \text{ cm}^2$	$Q_2$ $\mu\text{F cm}^{-2} \text{ Hz}^{1-n_2}$	$n_2$	$R_{ct}$ $\Omega \text{ cm}^2$	W $\Omega \text{ cm}^2$
0.5	0.01	6.94	0.74	926.8	740.2	0.61	2642	
1	2.01	39.2	0.56	823.6	222.6	0.92	1887	
2	3.25	22.3	0.83	694.8	400.2	0.78	1235	
3	2.58	18.6	0.85	756.8	364.2	0.65	1125	
4	8.34	25.3	0.67	627.8	563.2	0.74	596	
7	0.35	52.3	0.61	152.6	298.3	0.54	607.5	0.0114
9	0.26	68.6	0.49	102.7	131.2	0.56	569.5	0.0198
10	0.89	98.4	0.56	56.6	208.6	0.85	585.4	0.0286
12	1.25	37.2	0.54	48.9	156.4	0.92	574.6	0.0102
14	3.56	28.6	0.73	36.5	235.5	0.73	561.2	0.0035
17	0.25	26.3	0.68	26.3	115.2	0.65	512.5	0.0025
19	0.78	21.3	0.56	21.6	105.6	0.91	456.4	
21	0.56	15.6	0.68	15.3	103.6	0.64	402.6	
23	0.32	12.3	0.86	18.6	85.3	0.56	376.2	
28	0.56	9.62	0.64	12.3	56.2	0.74	312.5	

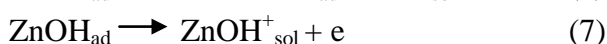
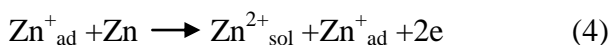
**Table 4.** The electrochemical parameters of the EIS in chloride-free SRL solution with different time

T days	$R_s$ $\Omega \text{ cm}^2$	$Q_1$ $\mu\text{Fcm}^{-2} \text{Hz}^{1-n_1}$	$n_1$	$R_f$ $\Omega \text{ cm}^2$	$Q_2$ $\mu\text{Fcm}^{-2} \text{Hz}^{1-n_2}$	$n_2$	$R_{ct}$ $\Omega \text{ cm}^2$	L $\text{H cm}^2$
0.25	198	214.3	0.64	692.4	87.2	0.78	954.2	1.58
0.5	208	201.2	0.92	923.1	41.3	0.65	1999	7.71
1	175	238.7	0.78	1294	22.9	0.79	2658	4.35
4	198	203.2	0.78	2323	18.6	0.68	2465	2.31
7	247	301.2	0.73	2340	19.9	0.78	2250	
9	211	286.3	0.69	2412	10.6	0.91	2362	
12	186	245.6	0.83	2198	8.6	0.86	2486	
14	223	290.3	0.81	2155	3.5	0.71	2540	
17	203	263.5	0.62	2596	5.6	0.68	2789	
21	172	240.3	0.82	2585	2.9	0.81	2945	
23	209	102.3	0.86	2613	5.6	0.69	2869	
28	183	86.3	0.78	2689	2.4	0.75	3102	

In the chloride-free SRL solution, the impedance spectra measured in the initial stages (6h~24h) exhibited a tail corresponded to the inductive loop in the low frequency region, indicating that intermediates species adsorbed on the electrode surface. According to the mechanism proposed by Cachet et al [18], dissolution of zinc in aqueous solution depends on the adsorbed intermediate species ( $\text{Zn}_{ad}^+$ ,  $\text{Zn}_{ad}^{2+}$  and  $\text{ZnOH}_{ad}$ ) as followed:



Therefore, the intermediates species adsorbed on the electrode surface play a “self -catalytic” role in the corrosion of zinc coating:



The adsorbed species, such as  $\text{Zn}_{ad}^+$ ,  $\text{Zn}_{ad}^{2+}$  and  $\text{ZnOH}_{ad}$ , could be the reason to the low frequency inductive loop.

The inductive loop disappeared (after 1 day) and both of the  $R_f$  and  $R_{ct}$  progressively increased with the increase of the immersion time (7-21 days). The changes in the impedance spectra in both size

and shape, combined with the increase in the capacitive loop in size, indicating that the rust layer was thickened and the protection afforded by the rust layer was improved in the SRL solution.

### 3.3.2 In SRL solution containing 3.5 wt % NaCl

In SRL solution containing 3.5 wt % NaCl, there are two capacitive loops in the Nyquist plots in the initial stage (12h ~2 day), corresponding to the two peaks on the  $\phi$ -log f curve in the Bode plot (Fig.4), indicating that two time constants existed at the initial stage of experimental system, the high frequency capacitance corresponds to the electrode surface rust layer film resistors and capacitors, low frequency capacitance corresponds to the charge-transfer behavior between the zinc coating interface and the solution.

The impedance measured during 7~14 days exhibited a tail corresponded to the Warburg impedance in the low frequency region of the Nyquist plots, indicating that a diffusion-controlled field existed on the surface of the specimen. This diffusion process can be attributed to the diffusion of oxygen based on the combined results of EIS and the above-mentioned polarization curves. Thus, the corrosion process was controlled by the cathodic reaction progress and the rate-determining step was transformed from charge transfer progress into oxygen diffusion controlling, as evidenced by the appearance of the Warburg in the Nyquist plots. With time (21 ~ 28 days), the Warburg impedance disappeared, both of the two capacitive loop decreased in size, and the value of  $R_f$  was decreased from  $926.8 \Omega \text{ cm}^2$  to  $12.3 \Omega \text{ cm}^2$ , which implied that the rust layer absorbed on the electrode surface damaged because of the  $\text{Cl}^-$  erosion.

As we know, by definition of the polarization resistance ( $R_p$ ),  $R_p$  is equal to  $(Z_F)_{\omega=0}$ , where  $Z_F$  is the faradaic impedance,  $\omega$  is the angular frequency. As  $\omega=0$ ,  $R_p = R_s + R_{ct} + R_f$  [29]. In the current study, the reciprocal of  $R_p$  (but not that of  $R_{ct}$ ) is used to characterize the corrosion rate because of its close relation to the SRL solution. Fig.6 shows the time dependence of the  $1/R_p$  of the galvanized steel under 3.5wt% NaCl SRL and chloride-free solution. It can be seen that the corrosion rate of galvanized steel increased abruptly during the initial immersion time(1~7 days), indicating that a breakdown of the rust layer under the erosion of  $\text{Cl}^-$ ; the corrosion process was controlled by the cathodic reaction (oxygen diffusion) during the 7~14 days, but the rate-determining step of corrosion was transformed from an oxygen diffusion to charge transfer progress, as evidenced by the disappearance of Warburg diffusion; the corrosion rate reached to the maximum during the 14~28 days, indicating that the rust layer was completely damaged. This trend is consistent with that of the polarization curves, and a similar phenomenon was also observed by Cao et al [33]. However, the corrosion rate of galvanized steel in chloride-free SRL solution decreased in the whole stages, that is to say, a protective rust layer absorbed on the electrode surface could improve the corrosion resistance of zinc coating. This phenomenon also could be explained in the following SEM images in Fig.7.

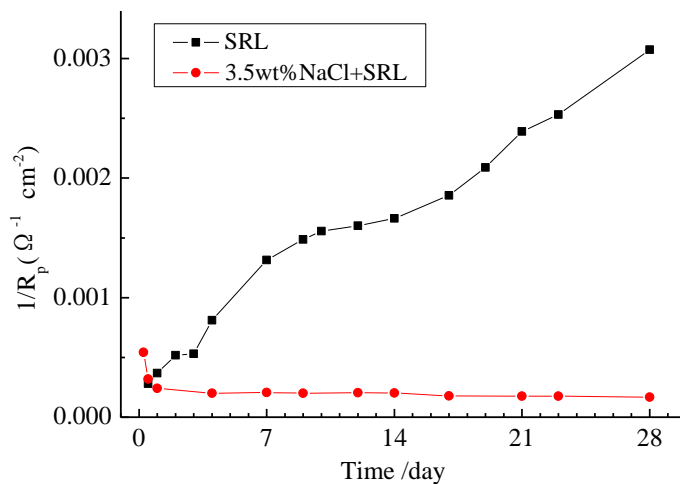


**Figure 6.** The time dependence of the 1/R<sub>p</sub> under 3.5wt% NaCl and chloride-free SRL solution

According to the above discussion, it is clear that the corrosion resistance of galvanized steel in chloride-free SRL solution is significant different from that under the SRL solution containing 3.5wt% NaCl.

### 3.4 Characterization

SEM, EDS and XRD characterizations are performed to investigate further the corrosion behavior of galvanized steel under 3.5wt% NaCl and chloride-free SRL solutions.

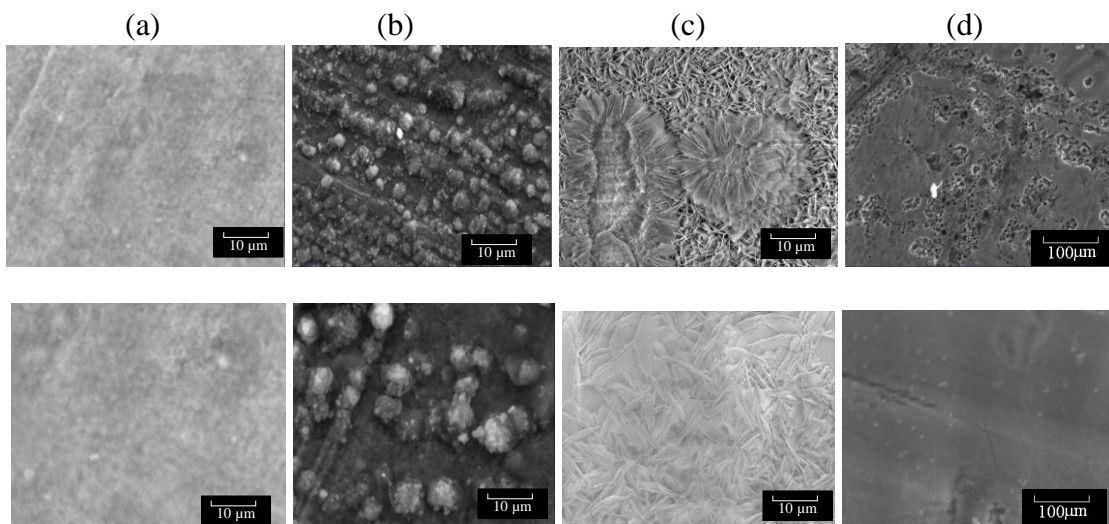


**Figure 7.** The SEM images of galvanized steel in 3.5wt% NaCl SRL solution (in upper row) and SRL solution (in lower row) for different immersion times: (a) before immersion; (b) 1 day; (c) 14 days; (d) 28 days (rust layer was scraped from the electrode surface)

The corrosion processes of the galvanized steel changed differently under 3.5wt% NaCl and chloride-free SRL solutions. Fig.7 shows the SEM images in different sampling time intervals. Fig.7 (a) presented the SEM images of the as-received sample of galvanized steel before the tests. This images presented here were for comparison with those of corroded samples. Evidently, the zinc coatings were compact, smooth and completely covered the substrate surface, no corrosion was found before the immersion on the electrodes surface; loose corrosion products absorbed on the electrode surface under both of the chloride-free and 3.5wt% NaCl SRL solutions after 1 days (Fig. 7(b)); when the time elapsing, pitting corrosion occurred obviously on the galvanized steel after 14 days (Fig.7 (c)) under the SRL solution containing 3.5wt% NaCl, and non-uniform corrosion occurred on the galvanized steel after removing the rust layer. These results were consistent with that of the EIS results as shown in Fig.4 and further supported the assumption of the oxygen diffusion control step. With time, the rust layer absorbed on the electrode was gradually damaged under the erosion of Cl<sup>-</sup>. However, lots of needle-like rust layer was adherent and compactly absorbed on the electrode surface under chloride-free SRL solution, the color of the surface became murky gray and little pitting corrosion was found on the zinc coating after removing the rust layer (Fig.7 (d)).

Fig.8 shows the EDS results of the chemical composition of the rust layer on the galvanized steel under 3.5wt% NaCl and chloride-free SRL solutions after 28 days of immersion. Obviously, Fe and Cl element were detected under the SRL solution containing 3.5wt% NaCl, indicating that zinc coating was damaged under Cl<sup>-</sup> erosion.

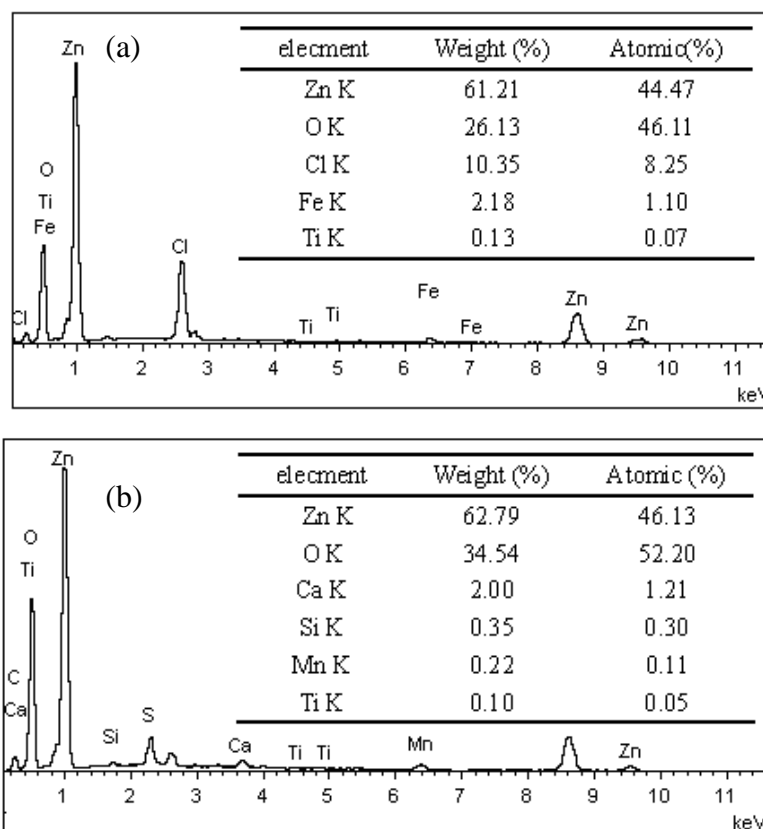


**Figure 8.** EDS results of the pitting corrosion area on galvanized steel under 3.5wt% NaCl (a) and chloride-free (b) SRL solution

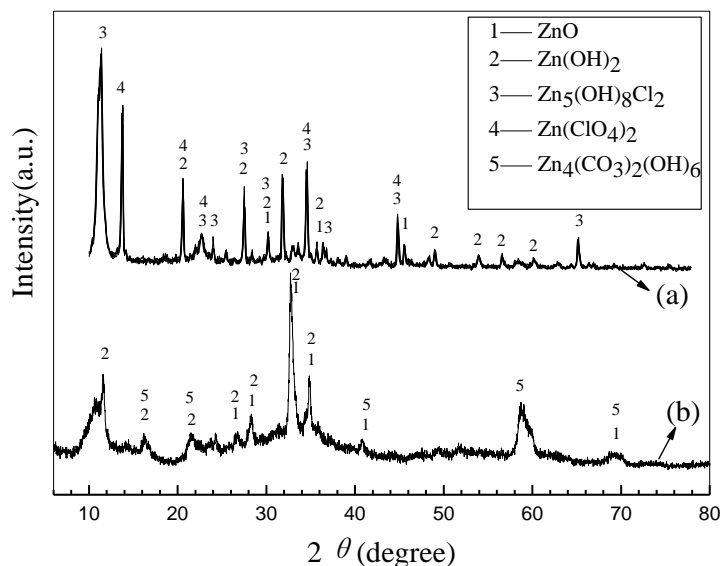


**Figure 9.** XRD spectra of the rust layer absorbed on galvanized steel under 3.5wt% NaCl (a) and chloride-free SRL (b) solution

In the chloride-free SRL solution, carbon element was detected and oxygen amounts of the rust layer increased compared with that under SRL solution containing 3.5wt% NaCl, indicating that the protective effects afforded by rust layer were zinc hydroxyl carbonate  $Zn_5(OH)_6(CO_3)_2$  and ZnO, which were in accordance with the followed XRD results.  $Zn_5(OH)_6(CO_3)_2$  could provide good protection of the zinc coating, which accounted for the good corrosion resistance of galvanized steel in SRL solution. A similar phenomenon was also observed by Chen [34].

Fig. 9 shows the XRD spectra of the rust layer absorbed on galvanized steel under 3.5wt% NaCl and chloride-free SRL solution for 28 days. The assignment was carried out by using the JCPDS database. The main products in SRL solution containing 3.5wt% NaCl were  $Zn_5(OH)_8Cl_2$ ,  $Zn(ClO_4)_2$ ,  $Zn(OH)_2$  and ZnO. It implied that the  $Cl^-$  played a role not only as a catalyst but also a reactant. In the chloride-free SRL solution, ZnO,  $Zn(OH)_2$ , and  $Zn_5(OH)_6(CO_3)_2$  were detected on the electrode surface. The peaks of  $Zn(OH)_2$  in both chloride-free and 3.5% NaCl SRL solutions were shallow and sharp, i.e.,  $Zn(OH)_2$  is thermodynamically stable in SRL solution encountered in this work.

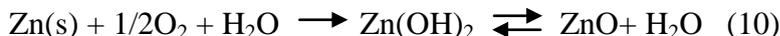
### 3.5 Mechanisms of the galvanized steel under SRL solution

The analysis carried out by XRD and EDS spectroscopy showed that the composition of the rust layer formed on the galvanized steel is quite complex under 3.5wt% NaCl and chloride-free SRL solution.

Corrosion of the zinc coating begins with the dissolution of zinc at anodic zone in aqueous solution, which depends on three different intermediates corresponding to the reaction (1~8). The anodic oxidation is balanced by an oxygen reduction reaction (9) at cathodic zone in alkaline medium.



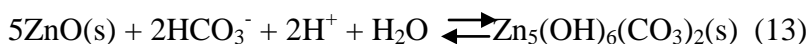
The initial rust layer was generated by the reaction of  $\text{OH}^-$  and  $\text{Zn}^{2+}$ . The over all reaction are given by (10)



ZnO is considered a semiconductor which has a low electronic conductivity, hence it may improve the corrosion resistance of zinc coating in alkaline environment [35].  $\text{Zn}_5(\text{OH})_6(\text{CO}_3)_2$  was detected by XRD after 28 days of immersion (Fig.9). As we know, increasing the pH value caused increased the dissolution of  $\text{CO}_2$  in the corrosive medium [36].



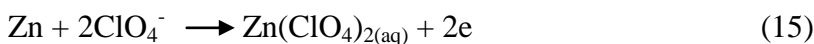
Alkaline conditions (i. e. availability of  $\text{OH}^-$ ) displaced (11) to the right. As more  $\text{CO}_2$  is supplied to the alkaline medium, The  $\text{CO}_3^{2-}$  further to produce hydrogen carbonate (12) and a resultant decrease in pH. The reaction is given by (13)



Pitting corrosion is a very complex phenomenon that potential involves several initial factors, including  $\text{Cl}^-$  concentration, pH value, temperature, and other variables.  $\text{Cl}^-$  is one of the important factors of zinc coating and a strong anodic activator [29]. The cyclic polarization measurement revealed that the  $\text{Cl}^-$  induced the pitting corrosion on zinc coating. In the presence of NaCl,  $\text{Cl}^-$  migrated to the anodic site [37] where  $\text{Zn}_5(\text{OH})_8\text{Cl}_2$  is formed according to (14), as described by Li[38].



$\text{Zn}_5\text{Cl}_2(\text{OH})_8$  is thermodynamically unstable at high alkalinity and prone to form ZnO. So, some crevices are formed and the released  $\text{Cl}^-$  could react with the zinc coating directly, resulting the compact rust layer damaged under the erosion of  $\text{Cl}^-$ . The  $\text{Zn}(\text{ClO}_4)_2$  detected by XRD in the present of NaCl also play a important role on the breakdown of the rust layer. According to Hassan [39] who studied the corrosion behavior of zinc in  $\text{ClO}_4^-$  solution, the  $\text{Zn}(\text{ClO}_4)_2$  was formed according to (15):



Above a certain concentration, the absorbed  $\text{ClO}_4^-$  ions became incorporated in the rust layer and subsequently participated in active anode dissolution, the rust layer break down under the influence of an electric field across the rust layer/solution interface[40].

#### 4. CONCLUSIONS

A comparative study of the corrosion behavior of galvanized steel under 3.5wt% NaCl and chloride-free simulated rust layer (SRL) solution was investigated by electrochemical measurements. The results showed that  $\text{Cl}^-$  could destroy the rust layer and increase the corrosion rate of the galvanized steel in SRL solution. These results were confirmed by XRD and EDS. A morphological study using SEM revealed that the needle-like rust layer was adherent and compactly absorbed on the electrode surface under chloride-free SRL solution, which could inhibit the diffusion of the oxygen and then improve the corrosion resistance of the galvanized steel. However, in the SRL solution containing 3.5wt% NaCl, the rust layer absorbed on the galvanized steel was gradually damaged under the erosion of  $\text{Cl}^-$ , the corrosion potential shifted towards cathodic values and the corrosion current increased with time, non-uniform corrosion occurred on the galvanized steel. The protective effects provided by the rust layer were destroyed by the erosion of  $\text{Cl}^-$  in SRL solution.

#### ACKNOWLEDGEMENT

The authors wish to acknowledge the financial support of the National Science Foundation of China (No.41076046).

#### References

1. El-Sayed M. Sherif, A. A. Almajid, A. K. Bairamov, Eissa Al-Zahrani. *Int. J. Electrochem. Sci.*, 7 (2012) 2796-2810
2. A.P. Yadav, H. Katayama, K. Noda, H. Masuda, A. Nishikata, T. Tsuru, *Electrochem. Acta.*, 52 (2007) 3121-3129.
3. M. A. Amin, H. H. Hassan, S. A. Rehim, *Electrochem. Acta.*, 53 (2008) 2600-2609.
4. B. L. Lin, J.T. Lu, G. Kong, *Corros. Sci.*, 4 (2008) 962-967.
5. J.B. Bajat, S. Stanković, B.M. Jokić, S.I. Stevanović, *Surf. Coat. Technol.*, 204 (2010) 2745-2753.
6. I.A. Kartsonakis, A.C. Balaskas, E.P. Koumoulos, C.A. Charitidis, G.C.Kordas, *Corros. Sci.*, 57 (2012) 30-41.
7. X.G. Zhang, Corrosion of zinc and zinc alloys, *Corrosion: Materials*, ASM Handbook, 2005, p.402-406.
8. M. Zapponi, T. Pérez, C. Ramos, C. Saragovi, *Corros. Sci.*, 47 (2005) 923-936.
9. N.S. Azmat, K.D. Ralston, B.C. Muddle, I.S. Cole, *Corros. Sci.*, 53 (2011) 1604-1615.
10. A.P. Yadav, A. Nishikata, T. Tsuru, *Corros. Sci.*, 46 (2004) 169-181.
11. M. Mokaddem, P. Volovitch, K. Ogle, *Electrochem. Acta.*, 55 (2010) 7867-7875.
12. T.N. Vu, M. Mokaddem, P. Volovitch, K. Ogle, *Electrochem. Acta.*, 74 (2012) 130-138.
13. Y. Zou, J. Wang, Y.Y. Zheng, *Corros. Sci.*, 53 (2011) 208-216.
14. J.Z. Duan, S.R. Wu, X.J. Zhang, G.Q. Huang, M. Du, B.R. Bao, *Electrochim. Acta.*, 54 (2008) 22-28
15. L. Bousselmi, C. Fiaud, B. Tribollets, E. Triki, *Corros. Sci.* 39 (1997) 1711-1724.

16. L.Yu, J.D. Duan, W. Zhao, Y.L. Huang, B.R. Hou. *Electrochem. Acta.*, 56 (2011) 9041-9047.
17. Tooru Tsuru. *Corros. Eng.* 59 (2010) 321-329.
18. C. Cachet, F. Ganne, G. Maurin, J. Petitjean, V. Vivier, R. Wiart, *Electrochem. Acta.*, 47 (2001) 509-518.
19. C. Cachet, F. Ganne, S. Joiret, G. Maurin, J. Petitjean, V. Vivier, R. Wiart, *Electrochem. Acta.*, 47 (2002) 3409-3422.
20. X. Zhang, S. L. Russo, A. Miotello, L. Guzman, E. Cattaruzza, P.L. Bonora, L. Benedetti, *Surf. Coat. Technol.*, 141 (2001) 187-193.
21. P. Volovitch, C. Allely, K. Ogle, *Corros. Sci.*, 51 (2009) 1251-1562.
22. N. Boshkov, K. Petrov, S. Vitkova, S. Nemska, G. Raichevsky, *Surf. Coat. Technol.*, 157 (2002) 171-178.
23. Z.I. Ortiz, P. Díaz-Arista, Y. Meas, R. Ortega-Borges, G. Trejo, *Corros. Sci.*, 51 (2009) 2703-2715.
24. C. Deslouis, M. Duprat, C. Tulet-Tournillon, *J. Electroanal. Chem.*, 181 (1984) 119-136.
25. N. Boshkov, *Surf. Coat. Technol.*, 172 (2003) 217-226.
26. H. Y. Sun, B. N. Zang, S. Liu, H. J. Fan, L. J. Sun, *Adv. Mater. Res.*, 399 (2012) 152-155.
27. S. Liu, H. Y. Sun, L.J. Sun, H.J. Fan. *Corros. Sci.*, 65 (2012) 520-527.
28. R. Lopes-Sesenes, G.F. Dominguez-Patiño, J.G. Gonzalez-Rodriguez, J. Uruchurtu-Chavarin. *Int. J. Electrochem. Sci.*, 8 (2013) 477-489
29. H. Zhang, X.G. Li, C.W. Du, H.B. Qi, *Int. J. Miner. Metall. Mater.*, 16 (2009) 414-421.
30. B. Zaid, D. Saidi, A. Benzaid, S. Hadji, *Corros. Sci.*, 50 (2008) 1841-1847.
31. D.C. Silverman, *Corrosion*, 48 (1992) 735-747.
32. H.L. Huang, Z.H. Dong, Z.Y. Chen, X.P. Guo, *Corros. Sci.*, 53 (2011) 1230-1236.
33. X.N. Liao, F.H. Cao, L.Y. Zheng, W.J. Liu, A.N. Chen, J.Q. Zhang, C.N. Cao, *Corros. Sci.*, 53 (2011) 3289-3298.
34. Y.Y. Chen, S.C. Chung, H.C. Shih, *Corros. Sci.*, 48 (2006) 3547-3564.
35. Y. Hamlaoui, L. Tifouti, F. Pedraza, *Corros. Sci.*, 52 (2010) 1883-1888.
36. M. Drogowska, L. Brossard, H. Menard, *J. Electrochem. Soc.*, 36 (1996) 217-225
37. Q. Qu, C. Yan, Y. Wan, C. Cao, *Corros. Sci.*, 44 (2002) 2789-2803.
38. Y. Li. *Corros. Sci.*, 43 (2001) 1973-1800
39. H.H. Hassan, *Appl. Surf. Sci.*, 174 (2001) 201-209.
40. T.P.Hoar, D. Mears, G. Rothwell, *Corros. Sci.*, 5(1965) 279-289.